Published in final edited form as:
Curr Biol. 2004 September 21; 14(18): 1685–1693. doi:10.1016/j.cub.2004.08.063.

Terminal Cytokinesis Events Uncovered after an RNAi Screen

Arnaud Echard[1,2,3], **Gilles R. X. Hickson**[1,3], **Edan Foley**[1,4], and **Patrick H. O'Farrell**[1,*]

[1] Department of Biochemistry and Biophysics, University of California, San Francisco, San Francisco, California 94143-2200

[2] Institut Curie, Centre National de la Recherche Scientifique, Unité Mixte de Recherche 144, 75248 Paris Cedex 5, France

Summary

Much of our understanding of animal cell cytokinesis centers on the regulation of the equatorial acto-myosin contractile ring that drives the rapid ingression of a deep cleavage furrow [1–5]. However, the central part of the mitotic spindle collapses to a dense structure that impedes the furrow and keeps the daughter cells connected via an intercellular bridge. Factors involved in the formation, maintenance, and resolution of this bridge are largely unknown [6]. Using a library of 7,216 double-stranded RNAs (dsRNAs) representing the conserved genes of *Drosophila*, we performed an RNA interference (RNAi) screen for cytokinesis genes in Schneider's S2 cells. We identified both familiar and novel genes whose inactivation induced a multi-nucleate phenotype. Using live video microscopy, we show that three genes: *anillin*, *citron-kinase (CG10522)*, and *soluble N-ethylmaleimide sensitive factor (NSF) attachment protein* (α-*SNAP*), are essential for the terminal (post-furrowing) events of cytokinesis. *anillin* RNAi caused gradual disruption of the intercellular bridge after furrowing; *citron-kinase* RNAi destabilized the bridge at a later stage; α-*SNAP* RNAi caused sister cells to fuse many hours later and by a different mechanism. We have shown that the stability of the intercellular bridge is essential for successful cytokinesis and have defined genes contributing to this stability.

Results and Discussion

Screening for Cytokinesis Genes

Although it narrows the waist of the cell, contraction of an internal acto-myosin ring is not sufficient to allow fusion of the opposing cellular membranes, a step required for the topological separation of daughter cells. Rather, as first described by Flemming in 1891 (see [7]), a persistent intercellular bridge forms around the spindle remnant; this bridge is marked at its center by a darkly staining structure, or midbody (e.g., Figure 1A, insert). This bridge remains long after furrowing has completed (see Figures 2A and 2B; see also Movies 1 and 2 in the Supplemental Data available with this article online), and micro-injection experiments in mammalian tissue culture cells have shown that it can allow the passage of molecules from

*Correspondence: ofarrell@cgl.ucsf.edu.
[3]These authors contributed equally to this work.
[4]Present address: Medical Microbiology and Immunology, University of Alberta, Edmonton, Alberta T6G 2H7, Canada.

Supplemental Data
Supplemental Data including detailed Experimental Procedures, a fully referenced version of Table 1 (Table S1), supplemental movies 1–11, and references are available at http://www.current-biology.com/cgi/content/full/14/18/1685/DC1/.

Note Added in Proof
As we were submitting this manuscript, there appeared a paper from the Glover laboratory describing *citron-kinase* mutant and RNAi phenotypes (D'Avino et al. [2004]. J. Cell Biol *166*, 61–71). However, this work did not follow cytokinesis to the stage of the late fusion, and it did not describe the events we report as the hallmark phenotype of Citron-kinase depletion.

one sister cell to the other, in some instances until the G2 phase of the next cell cycle [8]. Elegant EM studies revealed the bridge to be an elaborate structure containing anti-parallel microtubules embedded in the central electron-dense midbody [9,10]. The plasma membrane, tightly associated with microtubules along the length of the bridge, is highly fenestrated, and there are many vesicular structures within the bridge cytoplasm. Aside from these morphological data, very little is known about how an intercellular bridge is formed, stabilized, and eventually resolved to produce two topologically distinct cells (reviewed in [6]).

Recent advances in visualization technology, high-throughput analysis, and RNAi provide potent new tools for defining and exploring cell biological pathways. We have exploited these approaches to dissect steps in cytokinesis. From our screen of 7,216 dsRNAs (see [11] for library details), we visually identified and confirmed 30 dsRNAs that increase the incidence of multinucleate cells, an indicator of failed cytokinesis (Table 1 and Figure 1). Of these, 17 are newly implicated in *Drosophila* cytokinesis, and to our knowledge, 11 of these had not been previously implicated in animal cytokinesis (Tables 1 and S1). Additionally, five genes were identified through tests of candidate genes (asterisk in Table 1). The overlap with expectation is a testament to the specificity of the screen and the success of past efforts to define cytokinesis functions [2,4,5,12–16].

The largest category of genes (Tables 1 and S1) includes those previously implicated in contractile-ring formation/function, but some of these have unanticipated roles later in cytokinesis (e.g., *citron-kinase*, below). The second-largest category, harboring the most new genes, is composed of membrane trafficking genes such as regulators of SNARE-mediated membrane fusion (e.g., α-*SNAP*, below). A third category includes genes that contribute to the mitotic apparatus and hence may affect a precondition or regulatory input for cytokinesis (e.g., *fascetto*/PRC-1, our unpublished observations). There remain a number of diverse genes such as a highly conserved but uncharacterized cyclin-dependent kinase-related gene and genes influencing chromatin structure/function (Table 1).

Examination of the RNAi phenotypes in fixed cells (Figure 1) showed that some dsRNAs (e.g., *racGAP50C* or *pavarotti* kinesin; Figures 1B and 1C) blocked cytokinesis furrow ingression, as expected [16–19]. However, our attention was drawn to dsRNAs that did not block furrowing but nonetheless blocked cytokinesis, presumably at later, less-explored steps. Here we describe the phenotypic consequences of three such RNAi treatments: *anillin* (Figure 1D), *citron-kinase* (Figure 1E), and *soluble N-ethylmaleimide sensitive factor (NSF) attachment protein* (α-*SNAP*; Figure 1F).

Real-Time Records Highlight Late Events in Cytokinesis

To characterize the nature of the defects, we turned to live-cell video microscopy and first examined cytokinesis in cells expressing GFP-tubulin (Figure 2) or Histone H2B-GFP (data not shown). Control cells were round during metaphase and anaphase A (Figure 2A and Movie 1). As the spindle extended during anaphase B, the cells elongated nearly 2-fold. As cleavage furrow ingression proceeded, the spindle approached maximal extension and “central-spindle” fibers [1], which span the cell equator without reaching the poles, formed. During telophase nuclear reformation, these central-spindle fibers became highly compacted as they coalesced into a newly forming intercellular bridge (Figures 2A and 2B). As the cells progressed into interphase, they remained connected, but the tubulin content of the bridge steadily declined over a couple of hours, and GFP-tubulin became a less reliable marker of the bridge (Figure 2B and Movie 2). However, Anillin immunostaining served as an effective late marker of the bridge in fixed samples. Anillin concentrated in the cleavage furrow during anaphase and then in the intercellular bridge at telophase (Figure 3A), as previously reported [20]. With time, it became tightly compacted into a cortical ring encircling the bundle of microtubules at a position marked by a nadir in tubulin immunostaining; this nadir is known as the midbody (Figure 3A).

Surprisingly, as long as cells were gently processed for immunostaining, more than 60% of the cells were in pairs connected by these Anillin-positive cytokinetic bridges (Figures 3A and 3D). We conclude that intercellular bridges in S2 cells persist through much of the approximately 24 hr cell cycle and that the completion of cytokinesis (abscission) occurs many hours after mitosis.

Probing the Role of Actin in Intercellular Bridge Stability

Because the intercellular bridge is structurally sophisticated and long lasting, we expect many molecular events to contribute to its organization, maturation, and eventual resolution. We probed the role of actin in the maintenance of the bridge by using the inhibitor of F-actin assembly, Latrunculin A (LatA). LatA (1 μg/ml) prevented cleavage furrow formation, as expected, but did not cause all preexisting bridges to fail; even after 6 hr of treatment, many pairs of sister cells remained connected by Anillin-positive bridges (data not shown). We conclude that, at the concentration used, LatA blocks bridge formation but does not destabilize mature bridges. We then used video microscopy to monitor the effects of LatA administered during cytokinesis (Figures 2C and 2D; Movies 3 and 4). Whether added during furrowing (data not shown) or shortly thereafter (within 30 min; Figures 2C and 2D and Movies 3 and 4), LatA induced anomalies in the bridge 5–10 min later; the GFP-tubulin fluorescence started to decline more rapidly than normal, and the bridge started to progressively widen (Figure 2C). This led to gradual and slow (15–30 min) furrow regression in all cases when LatA was added during furrowing and in about half of cases when it was added shortly afterward. Importantly, when furrows regressed, there was no apparent dissociation of the plasma membrane from the microtubules within the bridge. Rather, the compacted bundle of microtubules lost coherency and progressively broadened in coordination with gradual widening of the bridge (arrow, Figure 2C). In the cases in which furrow regression was not observed, the decline in GFP-tubulin fluorescence was not accompanied by cleavage furrow regression within the time frame of the recordings (Figure 2D and Movie 3). From these analyses, we infer that bridge integrity graduates from sensitivity to 1 μg/ml LatA to resistance as bridges mature. We also conclude that maintenance of the compact structure of the microtubules of the bridge requires actin polymerization, whereas the attachment of the plasma membrane to the bridge can persist in its absence.

Stability of the Intercellular Bridge Requires Anillin

Because Anillin localizes to cleavage furrows, binds and bundles actin, and has a potential membrane binding PH domain, it has been proposed to link the contractile ring to the plasma membrane during cytokinesis [20–22]. Seemingly consistent with this notion, previous work showed that *anillin* RNAi induced extensive membrane blebbing in the cleavage area and resulted in cytokinesis failures as assessed in fixed preparations ([16]; see also Figure 1D, inset). Our real-time analysis has made it clear that the rampant membrane blebbing occurred *after* normal and complete cleavage furrow ingression and that cytokinesis failure is an even later event not associated with the onset of blebbing (Figure 2E, 00:05:30; also Movie 5). The aberrant membranous structures appeared to arise in association with dynamic microtubules that began invading the cortex (arrow in Figure 2E 00:10:00; also Movie 5). These perturbations occurred in the broad region flanking the furrow rather than at the bridge itself, where Anillin, and any remnants of the contractile ring, are ordinarily concentrated at this time (Figure 3A). We conclude that Anillin is required for stabilizing the cortex flanking the furrow (shortly after its ingression) and/or to regulate microtubule behavior at this location. This latter notion is supported by the finding that Anillin interacts with microtubules in addition to actin [23]. Although dramatic, this phase of membrane blebbing did not coincide with cytokinesis failure; the blebbing subsided, and a bridge with a compact bundle of microtubules formed relatively normally (Figure 2E, 00:36:30). Membrane blebbing finally resumed, but this time it was more global and encompassed the bridge region. The bundle of microtubules within the bridge began

to lose its integrity, the bridge broadened, and the cells fused (see Movie 5). As was seen after LatA treatment, cell fusion was a slow process (15–30 min), with full regression of the furrow being a late event after gradual disruption of the microtubules within the bridge. Based on this similarity, we suggest that the documented ability of Anillin to bundle actin is key to maintenance of the intercellular bridge at this stage. Although furrowing and initial elaboration of the bridge are relatively insensitive to Anillin depletion, our results suggest that Anillin has roles at several times during post-furrowing events in cytokinesis.

To better visualize the midbody, we observed the behavior of the kinesin-related protein Pavarotti-GFP (Pav-GFP), which specifically localized to the midbody matrix at the center of the bridge [24], where it persisted for several hours (Figure 4A and Movie 9). In *anillin* RNAi cells, the focus of Pav-GFP staining split into bundles that gradually separated from one another and slowly decomposed (Figure 4B and Movie 10). The multiple discrete foci that are seen for Pav-GFP staining during the breakup of the midbody recall the matrix material foci, known as stem bodies, that congregate during the formation of the midbody in mammalian cells. The dissociation of midbody structures coincided with disruption of the microtubule bundle visualized by GFP-tubulin (above) and with the gradual regression of the furrow. Thus, even though Anillin is localized to the central structure of the bridge, the compact midbody morphology, Pav-GFP localization (Figure 4B), and a gap in tubulin antibody staining show that the midbody still forms in Anillin-depleted cells. However, the subsequent destabilization of the midbody indicates that Anillin normally contributes to its stability or maturation. The relative timing of fusion of sister “cells” and the midbody disruption suggest that it is the lack of midbody stability that leads to cytokinesis failure upon depletion of Anillin function.

Stability of the Intercellular Bridge Requires Citron-Kinase

As with *anillin* RNAi, *citron-kinase* (CG10522) RNAi also produced a penetrant multinucleate phenotype (Table 1 and Figure 1E), although we found the nature of the defect to be distinct. Real-time analysis of GFP-tubulin revealed that cells progressed normally through mitosis, central spindle assembly, and cytokinesis furrow ingression (Figure 2F and Movie 6). At the conclusion of ingression, transient blebbing was observed and assessed as being more pronounced than similar blebbing in controls, but much less than in *anillin* RNAi. Otherwise, cell pairs appeared to progress normally as the bridge thinned and matured. However, 1–2 hr later, when the tubulin-GFP staining of the bridge was barely detectable, the cells abruptly merged over about 2 min (Figure 2F and Movie 6). We conclude that Citron-kinase is required for intercellular bridge stability, but at a much later stage than Anillin (compare bridge morphology in Figure 2F, 1:55:30, with that in Figure 2E, 00:36:30–00:50:30).

In the Pav-GFP-expressing cells (Figure 4C and Movie 11), *citron-kinase* RNAi did not initially affect the tight localization of the marker protein to the midbody, but about 5 min prior to fusion of the cells, the compact fluorescence split along the axis of the bridge into several distinct bundles of Pav-GFP. The initially subtle splitting progressed to more severe fragmentation over several minutes. When the cells fused, the membrane rapidly regressed, leaving foci of Pav-GFP in a central cluster (Figure 4C, 00:23:00–00:49:00). Apparently, the membrane lost attachment to the partially disrupted midbody structure (Figure 4C). Although *anillin* and *citron-kinase* RNAi each disrupted the midbody and destabilized the bridge, the *citron-kinase* RNAi phenotype had a distinctly later onset, the fusion event was faster, and the membrane regressed without a coordinate expansion of the midbody structure. Our results suggest that Citron-kinase has roles both in maintaining the assembly of midbody components and in coupling these structures to the membrane.

By immunofluorescence, we found that *citron-kinase* RNAi did not affect the formation of Anillin rings around the midbody in telophase cells (not shown, but as in Figure 3A). However, remnants of these rings were rarely observed in the resulting binucleate cells (10% after 3 d

RNAi, Figure 3C), whereas they frequently persisted in binucleate cells induced by α-*SNAP* RNAi (83%; see below and Figure 3E). Additionally, after *citron-kinase* RNAi, fewer mononucleate cells were connected as pairs joined by Anillin-positive bridges (approximately 10% versus >60% in controls, Figure 3D). We conclude that Citron-kinase is required for the stability of Anillin rings. Because the decrease in cell pairs did not lead to a coordinate increase in binucleate cells (Figure 3D), we also conclude that the destabilization of intercellular bridges induced by *citron-kinase* RNAi sometimes led to cell fusion and other times led to (premature) abscission.

Our findings with *citron-kinase* RNAi were unexpected; based on the fact that it interacts with Rho GTPase, localizes to cleavage furrows [25,26], and phosphorylates myosin light chains [27], it has been assumed to function primarily in acto-myosin ring contraction. Furthermore, overexpression of kinase-dead or truncated forms of Citron-kinase in mammalian cells induced aberrant contractions during furrowing [26]. However, consistent with the later roles we have uncovered, mammalian Citron-kinase localized to the midbody after furrowing [25,26] and to presumed midbody remnants in primary hepatocytes [28]. Also, Citron-kinase-deficient mice exhibited a highly penetrant cytokinesis failure in spermatogonial cells ([29] and references therein). The “division” of these cells is normally characterized by persistent intercellular bridges (that never seal) between sister cells. Thus, although the lack of embryonic lethality in these mice indicates that most cells had successfully undergone cytokinesis, a requirement for Citron-kinase in murine cell division is particularly obvious when resolution of intercellular bridges is slow (or absent). We, therefore, propose that Citron-kinase has roles in intercellular-bridge stability in diverse species.

Depleting α-SNAP Function Disrupts Intercellular Bridges

Although *citron-kinase* RNAi destabilized the bridges within a couple of hours of furrowing, even later events were revealed after RNAi of a completely novel cytokinesis gene, α-SNAP (Figure 1F). Although long treatment and high doses of α-SNAP dsRNA were cell lethal (Table 1) and produced early failures in cytokinesis (regression during or soon after furrowing, data not shown), shorter treatment (2 days) with lower doses (5 ng/μl) allowed cells to form intercellular bridges that matured normally and remained stable for many hours (up to more than 20) before abruptly regressing to form binucleate cells (Figure 2G and Movies 7 and 8). Prior to regression, the bridges were not easily discernible by either GFP-tubulin fluorescence or phase contrast microscopy. However, persistent connections were obvious from the fact that sister cells remained tightly juxtaposed, even when moving significantly within the field of view (as observed in controls). In many instances, one of a pair of sister cells gradually expanded while the other shrank, indicating significant transfer of material through an unsealed intercellular bridge during the 2–3 hr preceding regression (Figure 2G and Movies 7 and 8; see also Figure 3E). As mentioned above, Anillin immunofluorescence revealed that 83% of the resulting binucleate cells contained Anillin-positive midbody remnants: enlarged (or broken) ring-like structures that appeared to have been stretched considerably prior to regression (Figure 3E). Thus, α-SNAP depletion does not destabilize Anillin rings, at least not in the same manner as with *citron-kinase* RNAi. We conclude that an extremely late step in cytokinesis has a requirement for a particularly high level of α-SNAP function and that the affected step is distinct from that affected by depletion of Anillin or Citron-kinase. We note that all of the RNAi phenotypes we report, while defining a functional requirement for the gene we have targeted, are unlikely to define all the roles of the genes considered; some roles of a gene might be satisfied by low levels of residual gene function or performed by redundant gene function, or the phenotype induced by a deficit in a particular function might not be perceptible.

Although more work will be required to identify the basis for the late fusion of sister cells after α-*SNAP* RNAi, the essential role of α-SNAP in SNARE-mediated membrane fusion reactions

(see [30]) strongly reinforces the notion that membrane fusion is essential for the completion of animal cytokinesis [31–33], presumably through the sealing of the intercellular bridge. Our screen also uncovered syntaxin t-SNAREs and the SNARE complex regulator *Rop* (Table 1): other genes intimately involved in membrane fusion [30] and homologs of the *Arabidopsis* genes *KNOLLE* and *KEULE* that are required for plant cytokinesis [34]. Collectively, these data reinforce other suggestions that animal cell cytokinesis is more mechanistically akin to plant cytokinesis than originally thought [31–33].

The defects we have characterized by real-time analysis dramatize the importance of the post-mitotic intercellular bridge. Its formation, stability, and resolution are of paramount importance to the success of cytokinesis, and the identification of genes involved provide an entré e to molecular studies of these poorly understood processes.

Supplementary Material

Refer to Web version on PubMed Central for supplementary material.

Acknowledgments

The library of dsRNAs was produced in collaboration with the laboratories of Ron Vale and Grae Davis at the University of California, San Francisco. We thank colleagues for gifts of reagents (see Experimental Procedures) and Renny Feldman, David Morgan, Minx Fuller, and Yohanns Bellaiche for critically reading an early draft of the manuscript. A.E. thanks Bruno Goud for constant support and discussions and the Association pour la Recherche sur le Cancer (ARC grant 3269). Supported in part by a Herbert W. Boyer Postdoctoral Fellowship to G.R.X.H., by a Human Frontier Science Program Postdoctoral Fellowship to A.E., and by fellowship DRG1713-02 from the Damon Runyon Cancer Research Foundation to E.F. The research was supported by National Institutes of Health grants GM37193 and GM60988 to P.H.O'F.

References

1. Gatti M, Giansanti MG, Bonaccorsi S. Relationships between the central spindle and the contractile ring during cytokinesis in animal cells. Microsc Res Tech 2000;49:202–208. [PubMed: 10816260]
2. Glotzer M. Animal cell cytokinesis. Annu Rev Cell Dev Biol 2001;17:351–386. [PubMed: 11687493]
3. Goldberg, ML.; Gunsalus, KC.; Karess, RE.; Chang, F. Cytokinesis. In: Endow, SA.; Glover, DM., editors. Dynamics of Cell Division. Oxford, UK: Oxford University Press; 1998. p. 270-316.
4. Guertin DA, Trautmann S, McCollum D. Cytokinesis in eukaryotes. Microbiol Mol Biol Rev 2002;66:155–178. [PubMed: 12040122]
5. Prokopenko SN, Saint R, Bellen HJ. Untying the Gordian knot of cytokinesis. Role of small G proteins and their regulators. J Cell Biol 2000;148:843–848. [PubMed: 10704435]
6. Schweitzer JK, D'Souza-Schorey C. Finishing the job: cytoskeletal and membrane events bring cytokinesis to an end. Exp Cell Res 2004;295:1–8. [PubMed: 15051485]
7. Paweletz N. Walther Flemming: pioneer of mitosis research. Nat Rev Mol Cell Biol 2001;2:72–75. [PubMed: 11413469]
8. Schulze ES, Blose SH. Passage of molecules across the intercellular bridge between post-mitotic daughter cells. Exp Cell Res 1984;151:367–373. [PubMed: 6423396]
9. McIntosh JR, Landis SC. The distribution of spindle microtubules during mitosis in cultured human cells. J Cell Biol 1971;49:468–497. [PubMed: 19866774]
10. Mullins JM, Biesele JJ. Terminal phase of cytokinesis in D-98s cells. J Cell Biol 1977;73:672–684. [PubMed: 873994]
11. Foley E, O'Farrell PH. Functional dissection of an innate immune response by a genome-wide RNAi screen. PLoS Biol 2004;2(8):e203.10.1371/journal.pbio.0020203 [PubMed: 15221030]
12. Giansanti MG, Bonaccorsi S, Bucciarelli E, Gatti M. Drosophila male meiosis as a model system for the study of cytokinesis in animal cells. Cell Struct Funct 2001;26:609–617. [PubMed: 11942616]

13. Gonczy P, Echeverri C, Oegema K, Coulson A, Jones SJ, Copley RR, Duperon J, Oegema J, Brehm M, Cassin E, et al. Functional genomic analysis of cell division in C. elegans using RNAi of genes on chromosome III. Nature 2000;408:331–336. [PubMed: 11099034]

14. Pollard TD. Functional genomics of cell morphology using RNA interference: pick your style, broad or deep. J Biol 2003;2(25) Published online October 1, 2003. 10.1186/1475-4924-2-25

15. Skop AR, Liu H, Yates IJ, Meyer BJ, Heald R. Dissection of the mammalian midbody proteome reveals conserved cytokinesis mechanisms. Science 2004;305:61–66. [PubMed: 15166316]

16. Somma MP, Fasulo B, Cenci G, Cundari E, Gatti M. Molecular dissection of cytokinesis by RNA interference in Drosophila cultured cells. Mol Biol Cell 2002;13:2448–2460. [PubMed: 12134082]

17. Adams RR, Tavares AA, Salzberg A, Bellen HJ, Glover DM. pavarotti encodes a kinesin-like protein required to organize the central spindle and contractile ring for cytokinesis. Genes Dev 1998;12:1483–1494. [PubMed: 9585508]

18. Goshima G, Vale RD. The roles of microtubule-based motor proteins in mitosis: comprehensive RNAi analysis in the Drosophila S2 cell line. J Cell Biol 2003;162:1003–1016. [PubMed: 12975346]

19. Somers WG, Saint R. A RhoGEF and Rho family GTPase-activating protein complex links the contractile ring to cortical microtubules at the onset of cytokinesis. Dev Cell 2003;4:29–39. [PubMed: 12530961]

20. Field CM, Alberts BM. Anillin, a contractile ring protein that cycles from the nucleus to the cell cortex. J Cell Biol 1995;131:165–178. [PubMed: 7559773]

21. Giansanti MG, Bonaccorsi S, Gatti M. The role of anillin in meiotic cytokinesis of Drosophila males. J Cell Sci 1999;112:2323–2334. [PubMed: 10381388]

22. Oegema K, Savoian MS, Mitchison TJ, Field CM. Functional analysis of a human homologue of the Drosophila actin binding protein anillin suggests a role in cytokinesis. J Cell Biol 2000;150:539–552. [PubMed: 10931866]

23. Sisson JC, Field C, Ventura R, Royou A, Sullivan W. Lava lamp, a novel peripheral golgi protein, is required for Drosophila melanogaster cellularization. J Cell Biol 2000;151:905–918. [PubMed: 11076973]

24. Minestrini G, Harley AS, Glover DM. Localization of Pavarotti-KLP in living Drosophila embryos suggests roles in reorganizing the cortical cytoskeleton during the mitotic cycle. Mol Biol Cell 2003;14:4028–4038. [PubMed: 14517316]

25. Eda M, Yonemura S, Kato T, Watanabe N, Ishizaki T, Madaule P, Narumiya S. Rho-dependent transfer of Citron-kinase to the cleavage furrow of dividing cells. J Cell Sci 2001;114:3273–3284. [PubMed: 11591816]

26. Madaule P, Eda M, Watanabe N, Fujisawa K, Matsuoka T, Bito H, Ishizaki T, Narumiya S. Role of citron kinase as a target of the small GTPase Rho in cytokinesis. Nature 1998;394:491–494. [PubMed: 9697773]

27. Yamashiro S, Totsukawa G, Yamakita Y, Sasaki Y, Madaule P, Ishizaki T, Narumiya S, Matsumura F. Citron kinase, a Rho-dependent kinase, induces di-phosphorylation of regulatory light chain of myosin II. Mol Biol Cell 2003;14:1745–1756. [PubMed: 12802051]

28. Liu H, Di Cunto F, Imarisio S, Reid LM. Citron kinase is a cell cycle-dependent, nuclear protein required for G2/M transition of hepatocytes. J Biol Chem 2003;278:2541–2548. [PubMed: 12411428]

29. Di Cunto F, Imarisio S, Camera P, Boitani C, Altruda F, Silengo L. Essential role of citron kinase in cytokinesis of spermatogenic precursors. J Cell Sci 2002;115:4819–4826. [PubMed: 12432070]

30. Chen YA, Scheller RH. SNARE-mediated membrane fusion. Nat Rev Mol Cell Biol 2001;2:98–106. [PubMed: 11252968]

31. Finger FP, White JG. Fusion and fission: membrane trafficking in animal cytokinesis. Cell 2002;108:727–730. [PubMed: 11955425]

32. Straight AF, Field CM. Microtubules, membranes and cytokinesis. Curr Biol 2000;10:R760–R770. [PubMed: 11069103]

33. Xu H, Boulianne GL, Trimble WS. Membrane trafficking in cytokinesis. Semin Cell Dev Biol 2002;13:77–82. [PubMed: 12127139]

34. Assaad FF, Huet Y, Mayer U, Jurgens G. The cytokinesis gene KEULE encodes a Sec1 protein that binds the syntaxin KNOLLE. J Cell Biol 2001;152:531–543. [PubMed: 11157980]

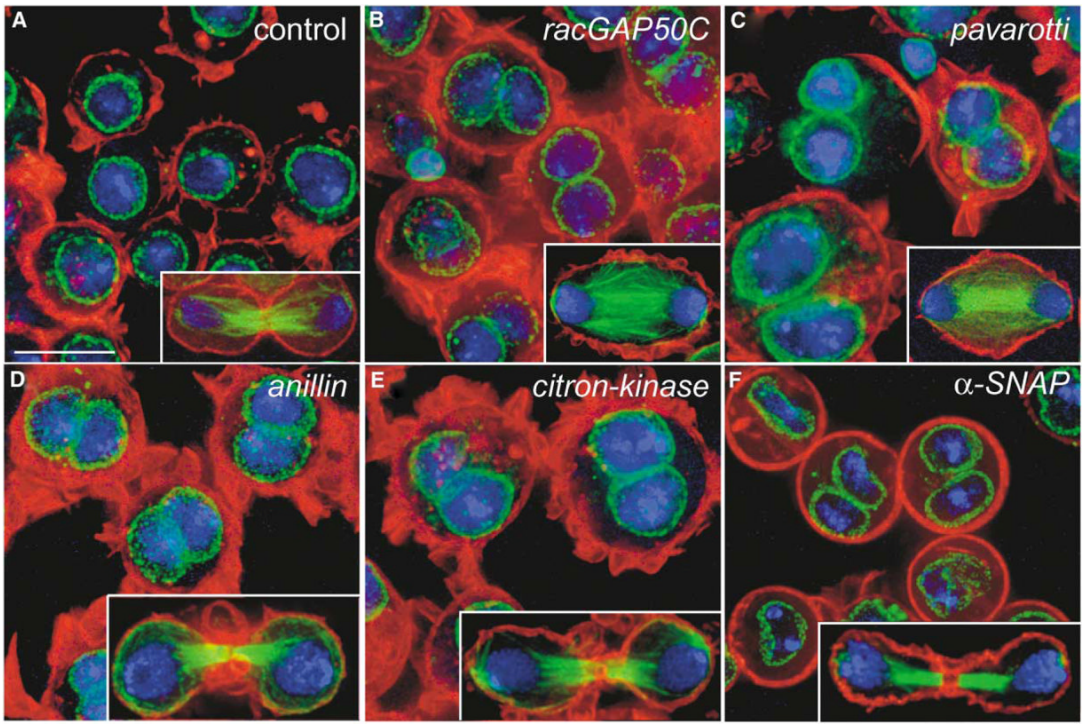

Figure 1. Cytokinesis Failure and the Multinucleate Phenotype Induced by *racGap50C, pavarotti, anillin, citron-kinase,* or α-*SNAP* RNAi

(A–F) S2 cells were fixed and stained for F-actin (phalloidin/red), nuclear envelope (wheat germ agglutinin/green), and DNA (Hoechst 33258/blue) (main panels) or for tubulin (green), F-actin (red), and DNA (blue) (insets). (A) Control; (B–E) 2–3 day treatment with dsRNA for (B) *racGap50C*, (C) *pavarotti*, (D) *anillin*, (E) *citron-kinase*, and (F) α-*SNAP*. RNAi of these genes induced multinucleate cells. The insets show late mitotic/telophase cells demonstrating furrowing in (A and D–F) and no furrowing in (B and C). The scale bar represents 10 μm.

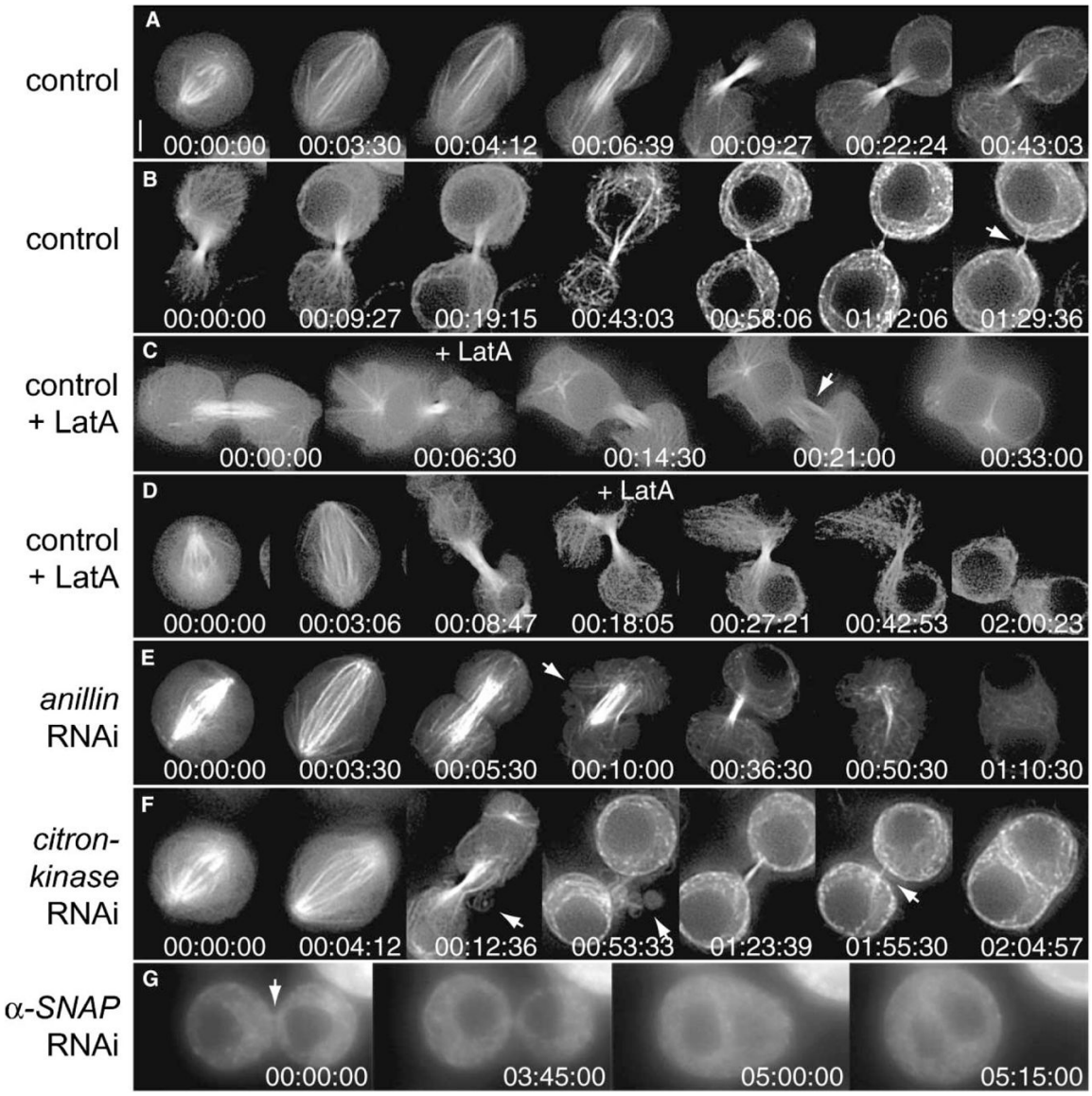

Figure 2. Video Microscopy of GFP-Tubulin in Control, Latrunculin A-Treated, and *anillin*, *citron-kinase*, or *α-SNAP* RNAi Cells Undergoing Cytokinesis

(A and B) Control cell illustrating anaphase spindle progression, cleavage furrow ingression, and formation of an intercellular bridge. In a longer record (B), the tubulin content of the bridge gradually declined, but the bridge was detectable for at least 1 hr 30 min (arrow). (C) Example of a control cell treated with the inhibitor of F-Actin assembly Latrunculin A (LatA; 1 μg/ml) added shortly (6 min 30 s) after furrowing. This disrupted the compact bundle of microtubules and resulted in widening of the bridge and gradual cleavage furrow regression. Note that during regression membrane attachment to the bridge did not appear to be compromised (arrow). (D) Example of a control cell where LatA was added slightly later (approximately 10 min) after furrowing. Although the tubulin content of the bridge began to decline more rapidly than usual (00:27:21 and 00:42:53) and the connection appeared to widen slightly, bridge integrity was maintained, and cell fusion was not observed within the 2 hr duration of the movie. (E) Two days of *anillin* RNAi. Anaphase cell elongation, central spindle formation, and furrow ingression proceeded normally (00:00:00–00:05:30). However, shortly after furrowing,

extensive membrane blebbing occurred in the cleavage area, associated with microtubules (arrow, 00:10:00). The blebbing subsided, and the microtubules compacted as an apparently normal bridge formed (00:36:30). Later, the microtubule bundle slowly dissociated, then gradually disintegrated amid renewed blebbing (00:50:30). Ultimately, the furrow slowly regressed to form a binucleate cell (01:10:30). (F) Three days of *citron-kinase* RNAi. The cell progressed normally through anaphase and telophase (00:00:00-00:12:36). Shortly after furrowing, initial elaboration of the intercellular bridge was marked by reversible membrane blebbing (arrows in 00:12:36 and 00:53:33; transiently—see movie S6—this blebbing was more pronounced than in controls but less than in *anillin* RNAi). Otherwise, the sister cells appeared normal as the intercellular bridge progressively thinned and matured (01:23:39–01:55:30). Eventually, when the bridge was barely still visible (arrow, 1:55:30), the cells abruptly merged (02:04:57). (G) Two days of α-*SNAP* RNAi. A faint connection is visible between a pair of sister cells at the start of the movie (00:00:00, arrow). By 03:45:00, the right-hand sister began to shrink as the left-hand one grew. Cell fusion occurred at 05:00:00, but note that the bridge was already mature by the start of the movie. Times are given as (hr:min:s) from the start of each sequence. The scale bar represents 3 μm. See the Supplemental Data for the movie files.

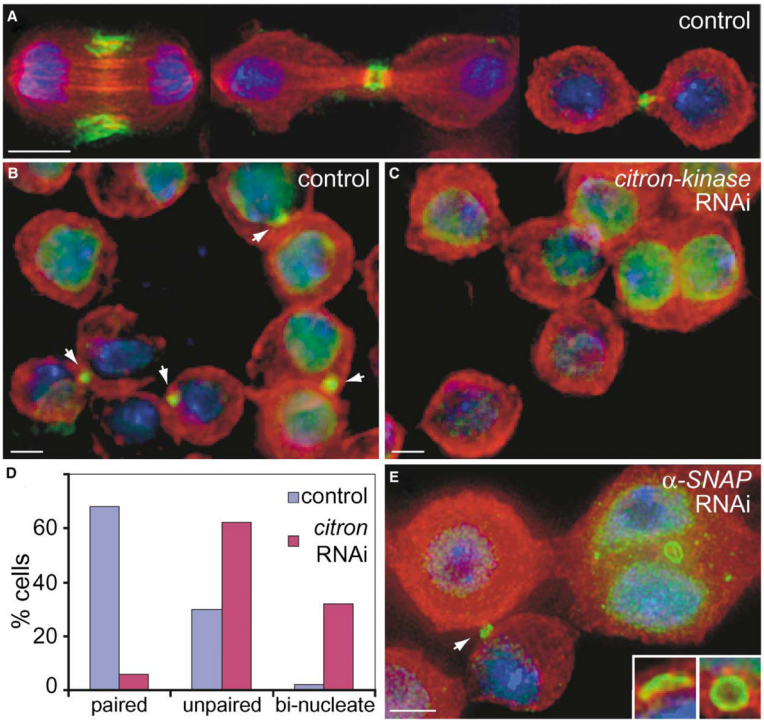

Figure 3. Anillin Localization in Control and *citron-kinase* or *α-SNAP* RNAi Cells

Cells were fixed and stained with Hoechst 33258 (blue) and antibodies to α-tubulin (red) and Anillin (green). (A) In control cells (no RNAi), Anillin localized to the cleavage furrow during anaphase (left panel), formed rings around the midbody matrix in telophase (center panel; note the gap in tubulin immunoreactivity), and persisted at this location into interphase (right panel). (B) Control cells (no RNAi) showing that Anillin-positive bridges connected pairs of cells throughout much of interphase (arrows). Note that Anillin accumulates in the nucleus as cells progress through interphase [20]. (C) Three days of *citron-kinase* RNAi. Although Anillin accumulated normally in interphase nuclei, and in telophase bridges (not shown), fewer interphase cells were connected by bridges. In addition, remnants of Anillin rings were rarely seen in binucleate cells after *citron-kinase* RNAi. (D) Quantification of paired cells in controls and after *citron-kinase* RNAi. After gentle transfer to conA-coated coverslips, cells were immunostained for Anillin and α-tubulin. Mononucleate cells that were paired (sister cells still connected by an Anillin-positive bridge) or unpaired (cells no longer connected by an Anillin-positive bridge) and binucleate cells were counted in controls (n = 255 pairs) and after 3 days of *citron-kinase* RNAi (n = 264 pairs). Plot shows the percent of cells in each category. (E) Two days of α-*SNAP* RNAi. Remnants of Anillin rings persisted in the binucleate cells after cytokinesis failure. These rings often appeared stretched or broken (insets). Note also the pair of cells separated by an Anillin ring (arrow); much of the contents of one sister appear to have been transferred to the other, as seen in the live movies, indicating that the bridge is unsealed. The scale bars represent 3 μm.

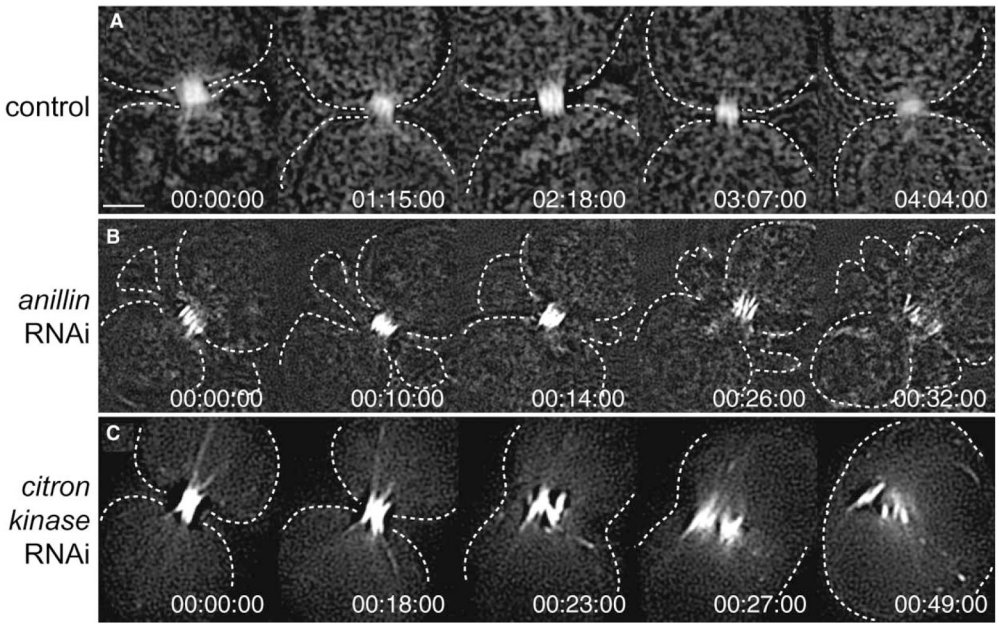

Figure 4. Video Microscopy of the Midbody Marker Pavarotti-GFP at Late Stages of Cytokinesis in Control and *anillin* or *citron-kinase* RNAi Cells

(A) A pair of sister cells connected by a bridge where Pav-GFP had concentrated into a compact structure that persisted throughout the 4 hr duration of the movie. Note that in this and subsequent movies, the cells had already completed furrow ingression at the time that the record was started and that the times do not correspond to the time after cytokinesis. (B) Two days of *anillin* RNAi. Amid rampant membrane blebbing, bundles of Pav-GFP fluorescence coalesced into a compacted midbody structure (00:10:00), although this gradually fragmented into the individual bundles as they decomposed (00:26:00–00:32:00). (C) Three days of *citron-kinase* RNAi. Bundles of Pav-GFP fluorescence began to split apart (00:18:00) and progressively separate as the plasma membrane rapidly regressed (00:23:00). However, the bundles remained loosely associated with one another and did not stay attached to the regressing membrane (00:27:00). Times are given as (hr:min:s) from the start of each sequence. The scale bar represents 2 μm. See the Supplemental Data for the movie files.

Table 1

A Genome-Wide RNAi-Based Screen Identified Both Familiar and Novel Cytokinesis Genes

	2° Tests		
Flybase Name (synonym/homolog)	**Screen**	**3 Days**	**6 Days**
Actin Ring Related			
racGAP50C	+++	+++	+++
pebble (Rho GEF)	+++	+++	+++
rho1	+++	++	+++
spaghetti squash (myosin II RLC)	+++	+++	+++
zipper (myosin II HC)	+++	++	+++
actin 5C	+++	na[#]	na[#]
actin 42A	+++	na[#]	na[#]
diaphanous (formin)	++	+	+++
peanut (septin)	++	+	+++
septin-2[*]	–	–	+++
scraps (anillin)[*]	–	+++	++^
twinstar (cofilin)	++	–	++
chickadee (profilin)[*]	–	–	++
citron kinase (CG10522)	+++	+++	+++
rok (rho-kinase)[*]	nd	+	+++
Membrane Trafficking/Organization			
α-SNAP	++	++	+
γ-*COP*	++	++	_^
rop (Sec1)	++	+	++
syntaxin 1A[*]	nd	–	+
syntaxin 5	+	–	++
sec5	+	–	+
CG3210 (Dynamin-2, Drp1)	+	–	++
fad2 (steroyl coA desaturase)	++	++	++^
cmp44E	+	–	++
Mitotic Spindle Related			
pavarotti (mitotic kinesin)	+++	+++	+++
fascetto (Ase1/PRC-1)	+++	+++	+++
α-*Tubulin at 84D*	+	++	^
Chromatin Regulators			
tra1 (TRRAP)	+	++	+++
caf-1 (chromatin assem. factor)	+	+	++
bap55	+	+	++^

	2° Tests		
Flybase Name (synonym/homolog)	**Screen**	**3 Days**	**6 Days**
cap-G (condensin)	+	+^	++^
Others			
ial (aurora B)	++	++^	++^
CG7236 (CDK-like, KKIALRE)	+	+	+++
polo kinase kinase 1	+	+	+
CG10068	+	−	+

Key: −, 0%–2% multinucleate cells;+, 5%–15% multinucleate cells; ++, 15%–30% multinucleate cells; +++, more than 30% multinucleate cells;

*, retested in candidate approach (not detected in screen; note that some of the candidates display cytokinesis defects only at day 6 and were thus nondetectable at the chosen screening time);

^, lethal/difficult to score; nd, not present in library and tested independently; and na#, not applicable (these cytoplasmic actins were recovered in the screen through cross-inactivation mediated via highly homologous dsRNAs and were subsequently found to act redundantly for cytokinesis; data not shown). Red entries are genes not heretofore implicated in animal cell cytokinesis (see Table S1 for details). Underlined entries are genes not heretofore implicated in *Drosophila* cytokinesis. Note that a control dsRNA (lacI) produced less than 2% multinucleate cells at all time points.